JOURNAL OF GENERAL VIROLOGY

RESEARCH ARTICLE

meng *et al.*, *Journal of General Virology* 2020;101:242–251

DOI 10.1099/jgv.0.001368

MICROBIOLOGY SOCIETY

OPEN MICROBIOLOGY

Identification of amino acid residues involved in the interaction between *peste-des-petits-ruminants* virus haemagglutinin protein and cellular receptors

Xuelian meng, Xueliang Zhu, Niyokwishimira Alfred and Zhidong Zhang*

Abstract

Peste-des-petits-ruminants virus (PPRV) haemagglutinin (H) protein mediates binding to cellular receptors and then initiates virus entry. To identify the key residues of PPRV H (Hv) protein of the Nigeria 75/1 strain involved in binding to receptors, interaction of the Hv and mutated Hv (mHv) proteins with receptors (SLAM and Nectin 4) and their mutants (mSLAM1, mSLAM2, mSLAM3 and mNectin 4) was investigated using surface plasmon resonance imaging (SPRi) and coimmunoprecipitation (co-IP) assays. The results showed that the Hv protein failed to interact with mSLAM3, but interacted at a strong or medium intensity with SLAM, mSLAM2, Nectin 4 and mNectin 4, and at a low level with mSLAM1. The mHv protein was unable to interact with SLAM and its mutants, but bound to Nectin 4 and mNectin 4 with medium and weak intensity, respectively. Further analysis showed that the Hv protein could precipitate mSLAM1, mSLAM2 and mNectin 4, but not mSLAM3. The mHv protein failed to coprecipitate with SLAM and its mutants. The binding activities of mNectin 4 and Nectin 4 to mHv were less than 30.36 and 51.94% of the wild-type levels, respectively. Based on the results obtained, amino acids at positions R389, L464, I498, R503, R533, Y541, Y543, F552 and Y553 of H protein and I61, H62, L64, K76, K78, E123, H130, I210, A211, S226 and R227 in SLAM were identified to be essential for the specificity of H–SLAM interaction, while the critical residues of H–Nectin 4 interaction require further study. These findings would improve our understanding of the invasive mechanisms of PPRV.

INTRODUCTION

Peste-des-petits-ruminants virus (PPRV) belongs to the genus *Morbillivirus* of the family *Paramyxoviridae*, along with measles virus (MV), Rinderpest virus (RPV) and canine distemper virus (CDV). PPRV causes an acute and severe contagious disease, *peste-des-petits-ruminants* (PPR) in small ruminants, particularly goats and sheep [1]. PPR was first reported in Africa in the 1940s, and has since shown a trend to spread. In addition to Africa, Asia and the Middle East, PPR has now reached Europe [2–6]. Following the successful eradication of Rinderpest, PPR has been targeted as the next candidate for global elimination by the World Organization for Animal Health (OIE) and the Food and Agriculture Organization (FAO) [6–9]. Viruses enters susceptible cells and initiate the subsequent infection events by specifically recognizing and binding receptors. Thus, the interaction between the viral proteins and receptors is the focus of virological study.

PPRV haemagglutinin (H) binding to receptors initiates the fusion of the viral membrane with the host cell membrane in the initial step of PPRV infection. The C-terminal ectodomain of PPRV H protein contains a membrane-proximal 96-residue stalk and a cuboidal 6-bladed β-propeller head domain that provide contact sites with the receptors [10–13]. Amino acids of MV H head domains are highly conserved and it is likely that H proteins of the other congeneric viruses may also utilize this region to infect cells. The virological data showed that amino acids 429–438 of MV H protein may be the functional domains interacting with signaling lymphocyte-activation molecule (CD150/SLAM) [14, 15].

Received 11 October 2019; Accepted 19 November 2019; Published 20 December 2019

Author affiliations: [1]State Key Laboratory of Veterinary Etiological Biology, Key Laboratory of Animal Virology of Ministry of Agriculture, Lanzhou Veterinary Research Institute, Chinese Academy of Agricultural Sciences, Xujiaping 1, Yanchangpu, Chengguan District, Lanzhou 730046, PR China.
***Correspondence:** Zhidong Zhang, zhangzhidong@caas.cn

Keywords: surface plasmon resonance imaging; co-immunoprecipitation assay; haemagglutinin (H); receptor; peste-des-petits-ruminants virus.

Abbreviations: CDV, canine distemper virus; co-IP, coimmunoprecipitation; Hv, hemagglutinin protein of PPRV strain Nigeria 75/1; mHv, site-directed mutant of PPRV Hv; mNectin 4, site-directed mutant of Nectin 4; mSLAMs, site-directed mutants of SLAM; MV, measles virus; Nectin 4, poliovirus receptor related 4; PPRV, *Peste-des-petits-ruminants* virus; RPV, rinderpest virus; SLAM, signaling lymphocyte-activation molecule; SPRi, surface plasmon resonance imaging; WT, wild-type.

Three supplementary figures are available with the online version of this article.

Recently, computational analysis results indicated that 21 amino acids at positions 191–196, 483 and 503–556 on MV and PPRV H proteins play a critical role in the H–SLAM interaction [12, 16]. Among these amino acids, amino acids at positions 503, 505, 507, 533, 543 and 552 were shared by human and ovine species for binding SLAM. Structurally, 22 amino acids in the 388–392, 458–506 and 524–550 domains of MV H showing strong attraction to human SLAM [11, 16] (Fig. S1, available in the online version of this article).

Cellular receptors determine the virus tropism and the host specificities. To date, two molecules, SLAM and poliovirus receptor-related 4 (Nectin 4/PVRL4) have been identified as receptors for PPRV [17, 18]. SLAM was also identified as a receptor for MV, CDV and RPV, while Nectin 4 for MV and CDV [19–22]. SLAM is expressed selectively in immune cells such as monocytes, dendritic cells and activated T and B cells [23–26]. SLAM contains an extracellular region with two Ig-like domains (V-C2 set). The V domain of SLAM is a critical domain for interacting with virus proteins and contains key sites specially binding to virus protein within spatial structures [27]. Hu *et al.* confirmed that amino acid 27–135 in the V domain was the functional domain that interacts with MV H [14] (Fig. S2). Ohishi *et al.* showed that eight (64, 67, 69, 73, 85, 119, 121 and 130) amino acid residues at positions 58–130 determined host–virus specificity and were shared by animal groups susceptible to the corresponding viruses in the genus *Morbillivirus* [28]. Molecular docking revealed the significance of 16 residues at positions 62–82, 123 and 127–131 of SLAM in determining caprine and human SLAM binding potentiality [12]. Intriguingly, amino acid residues at positions 58–63, 210–211 and 226–227 in human and ovine SLAM proteins have a key role in the receptor function of SLAM for PPRV and MV [14, 29, 30]. The 210, 211, 226 and 227 amino acids of ovine SLAM are I, A, S and R, respectively, different from the bovine, canine and human counterparts [31]. Nectin 4 is normally localized at adherent junctions and is expressed abundantly in epithelial cells [32, 33]. Nectin 4 contains three Ig-like ectodomains (V-C2-C2 sets), and has an important role in mediating cell–cell adhesion [34, 35]. The V domain of Nectin 4 is also involved in binding to viral proteins, serving as an entry factor [19, 36]. This receptor mediates virus infection in epithelial cells of the lungs and airways.

It is essential to accurately confirm the key amino acid residues mediating the interactional specificity of PPRV H and receptors in order to clarify viral invasion. The interactional amino acids between PPRV H and SLAM have been analysed based on a homology model of the complex. However, the key amino acid residues mediating the specificity of PPRV H interacting with the respective receptors remain largely unknown. Our previous study using surface plasmon resonance (SPR) determined the important heptad repeat region of PPRV F protein involved in intermolecular interaction in the fusion process [37]. Given these facts, in this study the recombinant plasmids expressing the wild-type (WT) and mutant receptors and PPRV H were constructed, and then SPR imaging (SPRi) and co-immunoprecipitation (co-IP) were applied to determine the key amino acids for the interactions between PPRV Hv and the receptors, SLAM and Nectin 4. The results showed that amino acids at positions R389, L464, I498, R503, R533, Y541, Y543, F552 and Y553 of PPRV Hv protein and I61, H62, L64, K76, K78, E123, H130, I210, A211, S226 and R227 in caprine SLAM determine the specificity of the H–SLAM interaction. The results should provide important information for developing peptide-based vaccines and antiviral drugs against PPR.

RESULTS

Preparation of the recombinant proteins

The recombinant expression vectors Hv-HA, mHv-HA, SLAM-Myc, Nectin 4-Myc, mSLAM1-Myc, mSLAM2-Myc, mSLAM3-Myc and mNectin 4-Myc were constructed successfully and transiently expressed in HEK293 cells. The results of SDS-PAGE (Fig. S3) and Western blot (Fig. 1) showed that target proteins with a high purity (>90%) and specificity could be used for SPRi.

Characterization of binding affinity by SPRi

Biotin (positive) and DMSO (negative) were used as system controls interacting with streptavidin to determine the quality of the chip. The results showed that the chip quality was good and it could be used for follow-up SPRi (Fig. 2).

The target proteins Hv-HA and mHv-HA were used as ligands and printed on the chip surface in quadruplicate. SLAM-Myc, Nectin 4-Myc, mSLAM1-Myc, mSLAM2-Myc, mSLAM3-Myc and mNectin 4-Myc were used as analytes and injected at different concentrations (200, 400, 800, 1600 and 3200 nM) on the same SPRi chip. The raw sensorgrams and measurements of the binding process of ligands and analytes were recorded in real time. The kinetic parameters, the association rate constant (k_a/k_{on}), the dissociation rate constant (k_d/k_{off}), and the equilibrium dissociation constant (K_D, k_d/k_a) were calculated to describe the protein–protein interactions from the sensorgrams (Table 1). The SPRi signal of protein–protein interactions increased with increasing protein concentration (Figs 3 and 4). The sensorgrams and affinity parameters showed that the interaction intensity of Hv with SLAM, Nectin4 and mNectin 4 was strong, while that with mSLAM2 was of medium intensity, and that with mSLAM1 and mSLAM3 was very weak or nonexistent (Fig. 3). The K_D value of Hv interacting with mSLAM2 was comparable to that for SLAM, while the K_D values for Hv interacting with mSLAM1 and mSLAM3 were much greater than that for SLAM, showing an approximately 10^3 to 10^4-fold difference. Moreover, the mHv protein did not interact with SLAM and its three mutants, but the interaction intensities of mHv with Nectin 4 and mNectin 4 were mild and weak, respectively (Fig. 4). The K_D value of mHv binding to SLAM and its three mutants was more than 10^{-2} M. he K_D value of Hv interacting with mNectin 4 was comparable to that for Nectin 4, while the K_D value of mHv interacting with Nectin 4 was much greater than the WT level, with an approximately 100-fold difference. The affinity of Hv–Hv or mHv–mHv interaction was caused by the formation of homodimers or tetramers. No

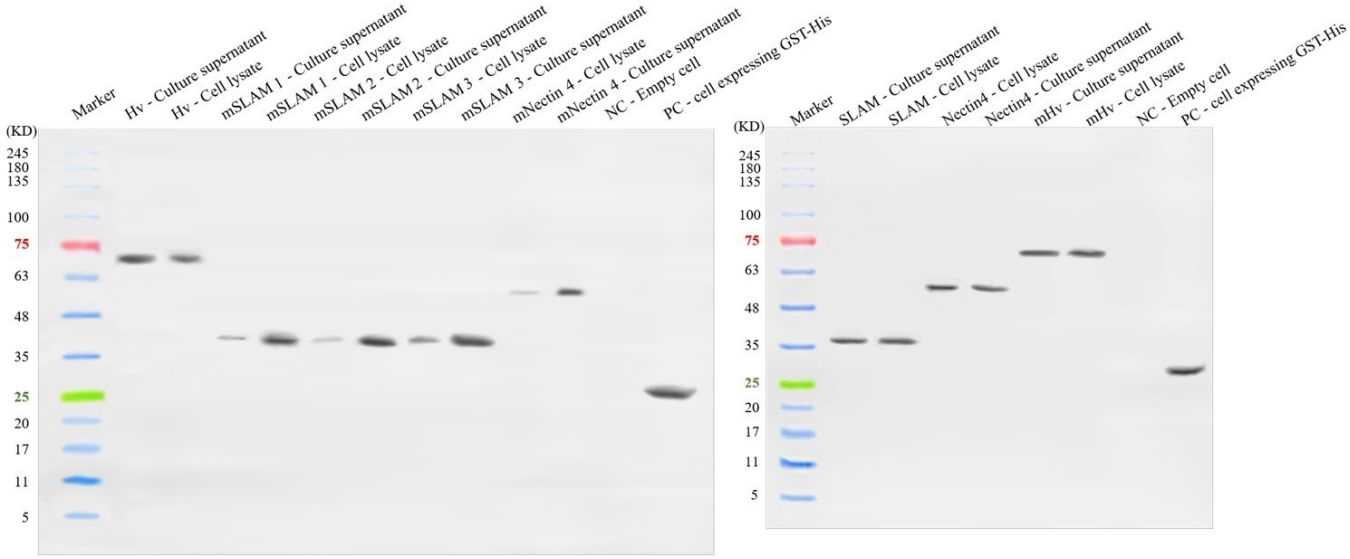

Fig. 1. Western blot of the recombinant protein.

binding was observed between Hv–PBS or mHv–PBS (Figs 3h and 4h).

These results indicated that the mutated amino acid residues of Hv, mSLAM1 and mSLAM3 are vital to the recognition and binding of the virus to SLAM. The mutated residues of Hv protein have an important effect on binding to Nectin 4, while the mutated amino acids sites of Nectin 4 may not play a decisive role in binding to Hv protein.

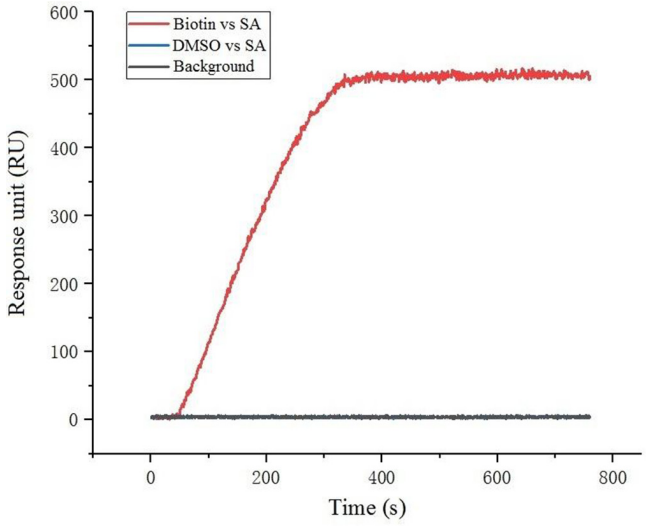

Fig. 2. Detection of microarray chip based on SPRi. SPRi graph showing interaction of biotin (positive control) and DMSO (negative control) with SA on the microarray chip.

Confirmation of binding affinity by co-immunoprecipitation assay

To further determine the key amino acid residues of Hv interacting with receptors, CHO cells co-transfected with different combinations of plasmids were subjected to immunoprecipitation, Western blot and grey value analysis by Alphaview SA. As shown in Fig. 5a, the Hv protein could not coprecipitate mSLAM3 and the mHv protein failed to coprecipitate SLAM and its three mutants. Although the Hv protein could coprecipitate mSLAM1 and mSLAM2, the interaction abilities were remarkably decreased, especially with mSLAM1, ranging from 36.99 to 55.07% of the WT level (Table 2). The results relayed in Fig. 5b and Table 3 showed that the binding activity of mNectin 4 to Hv remained above 70.5% of the WT level, while that of mNectin4 and Nectin 4 to mHv was less than 30.36 and 51.94% of the WT level, respectively. These results indicate that the mutated sites in mSLAM3 and mHv are the key amino acid residues for the interaction between SLAM and PPRV H protein, and the partially mutated residues in mSLAM1, mSLAM2 and mNectin 4 play key roles in receptors interacting with H, and the partially mutated residues of mHv are the critical sites for the interaction with Nectin 4.

Based on the results obtained, we identified that amino acids at positions R389, L464, I498, R503, R533, Y541, Y543, F552 and Y553 of PPRV H protein and I61, H62, L64, K76, K78, E123, H130, I210, A211, S226 and R227 in SLAM determine the specificity of the H–SLAM interaction.The key amino acids residues of PPRV H interacting with Nectin 4 could not be determined .

DISCUSSION

An accurate mechanism ensures timely and effective entry of viruses into host cells. PPRV H protein binding to viral

Table 1. Kinetic parameters of Hv and mHv proteins binding with receptors and mutants from SPRi

No.	analytes	ligands	Avg *ka*	Avg *kd*	Avg *KD*	Interactions	ABS (tr_*KD*)
			(1/Ms)	(1/s)	(M)	intensity	
1	SLAM	Hv	8.88E+02	9.59E-04	1.08E-06	Strong	19.8205
2	Nectin 4	Hv	1.42E+03	4.35E-04	3.06E-07	Strong	21.6395
3	mSLAM1	Hv	1.78E+01	5.06E-02	2.85E-03	Weak	8.4558
4	mSLAM2	Hv	8.45E+01	4.41E-03	5.22E-05	Middle	14.2250
5	mSLAM3	Hv	7.21E+00	2.34E-01	3.25E-02	VW/None	4.9432
6	mNectin 4	Hv	6.21E+02	1.11E-03	1.79E-06	Strong	19.0881
7	Hv	Hv	1.81E+01	5.14E-02	2.83E-03	Weak	8.4626
8	PBS	Hv	1.30E+00	2.80E-01	2.16E-01	VW/None	2.2111
9	SLAM	mHv	4.29E+00	1.33E-01	3.09E-02	VW/None	5.0177
10	Nectin 4	mHv	9.85E+01	2.08E-03	2.11E-05	Middle	15.5312
11	mSLAM1	mHv	5.64E+00	1.58E-01	2.80E-02	VW/None	5.1585
12	mSLAM2	mHv	1.37E+01	3.52E-01	2.56E-02	VW/None	5.2851
13	mSLAM3	mHv	2.99E+00	3.29E-01	1.10E-01	VW/None	3.1839
14	mNectin 4	mHv	1.81E+01	7.21E-02	3.99E-03	Weak	7.9697
15	mHv	mHv	1.87E+01	4.61E-02	2.47E-03	Weak	8.6604
16	PBS	mHv	1.95E+00	1.82E-01	9.33E-02	VW/None	3.4220

Interaction intensity level: 10^{-13}–10^{-8}, very strong; 10^{-8}–10^{-5},strong; 10^{-5}–10^{-3}, medium; 10^{-3}–2×10^{-2},weak; 2×10^{-2}–10^{2}, very week (VW)/ none). Avg k_a, average association rate constant; Avg k_d, average dissociation rate constant; Avg K_D, average equilibrium dissociation constant (k_d/k_a); ABS (tr_ K_D), absolute affinity coefficient [$\log_2(K_D)$].

receptors is the 'core' mechanism and an initial step for virus entry. Identification of the key amino acids of PPRV H involved in binding to cellular receptors is essential to understand the mechanism of virus entry. The H proteins of members of the family *Paramyxoviridae* have a globular head with a six-blade β-propeller structure that is responsible for receptor binding [11, 38–40]. A hydrophobic pocket of H protein is located at the boundary between blades β4 and

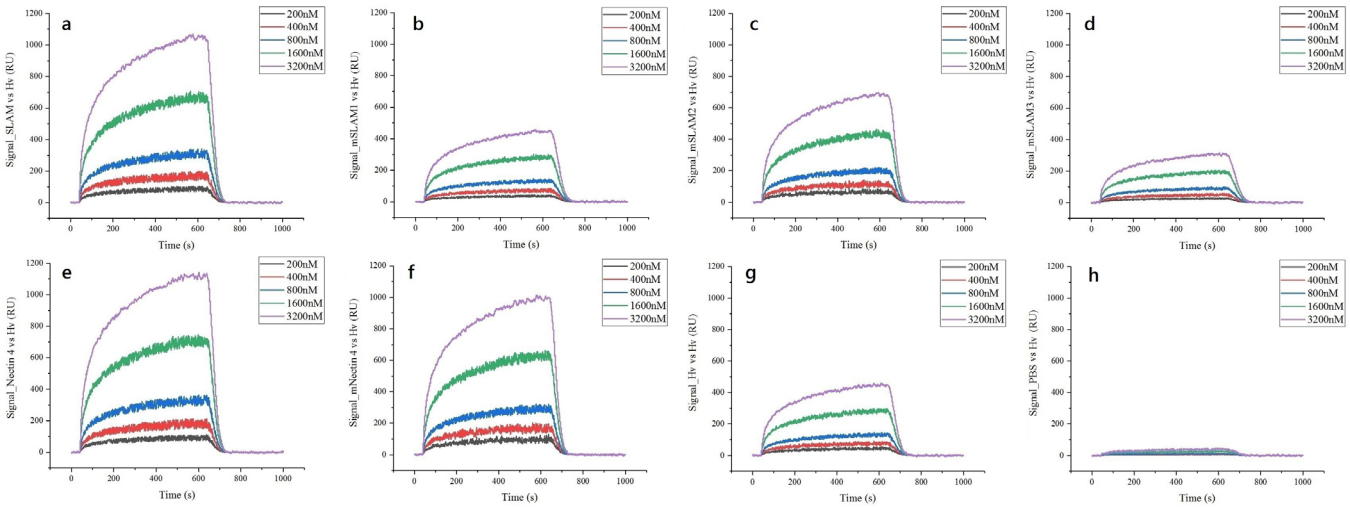

Fig. 3. SPR sensorgrams of the immobilized Hv–HA binding to the analytes at different concentrations (200, 400, 800, 1600 and 3200 nM). (a) SLAM–Myc. (b) mSLAM1–Myc. (c) mSLAM2–Myc. (d) mSLAM3–Myc. (e) Nectin 4–Myc. (f) mNectin 4–Myc. (g) Hv–HA. (h) PBS.

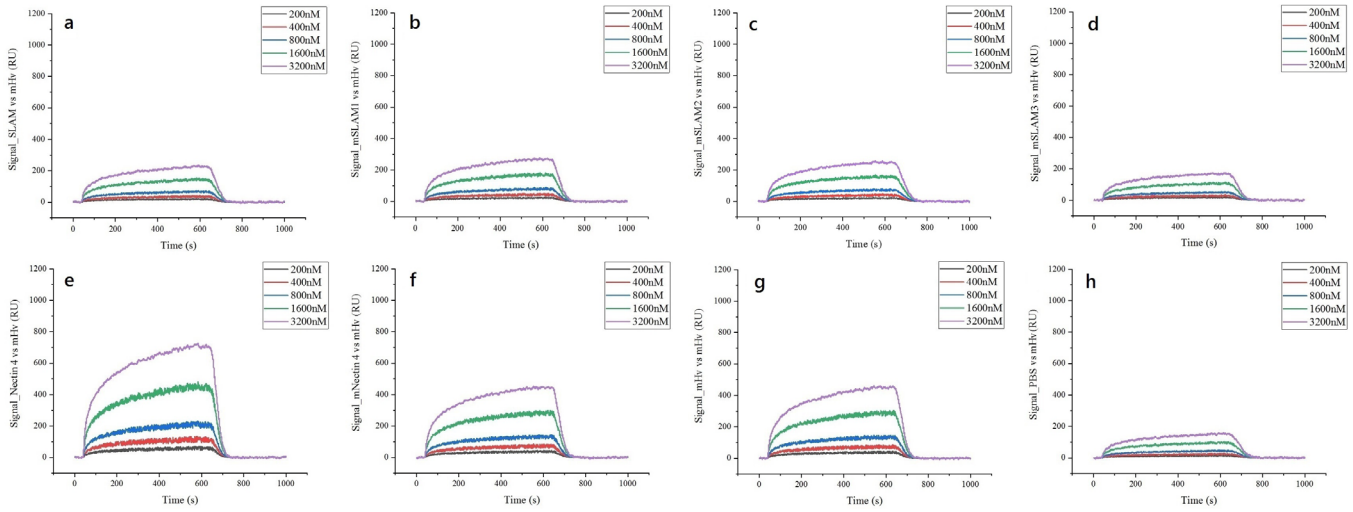

Fig. 4. SPR sensorgrams of the immobilized mHv-HA binding to the analytes at different concentrations (200, 400, 800, 1600 and 3200 nM). (a) SLAM–Myc. (b) mSLAM1–Myc. (c) mSLAM2–Myc. (d) mSLAM3–Myc. (e) Nectin 4–Myc. (f) mNectin 4–Myc. (g) mHv–HA. (h) PBS.

β5 and is involved in binding to receptors [12, 16]. Although the key sites of the MV H interfaces that bind to three receptors in the β4–β5 groove overlap somewhat, there are still considerable differences among the residues and structures of the MV H–receptor complexes [11–13, 41]. Several amino acid residues around the hydrophobic pocket in the β4 (residues 448–507) and β5 (residues 524–556) strand regions are essential for binding to the respective receptors. The PPRV Hv–shSLAM binding interface was consistent with that of the MV H–marmoset SLAM (maSLAM) complex [12, 16]. In this study, based on the virological and predictive reports, we constructed the WT and mutants of PPRV H and two receptors [14–16, 28, 29, 31]. Then we investigated the role of mutated amino acids residues in the PPRV H–receptor interactions by SPRi and co-IP.

The results of SPRi were consistent with those of co-IP in the present study. The PPRV H–mSLAM3 complex actually lost binding affinity, and the K_D value was far greater than that for Hv–SLAM, showing an approximately 10^4-fold difference. The Hv protein and mSLAM3 could not be coprecipitated. This indicated that the mutated amino acids (H62A, L64N, K76A, K78A, E123A and H130A) in mSLAM3 play a vital role in the PPRV H–SLAM interaction,

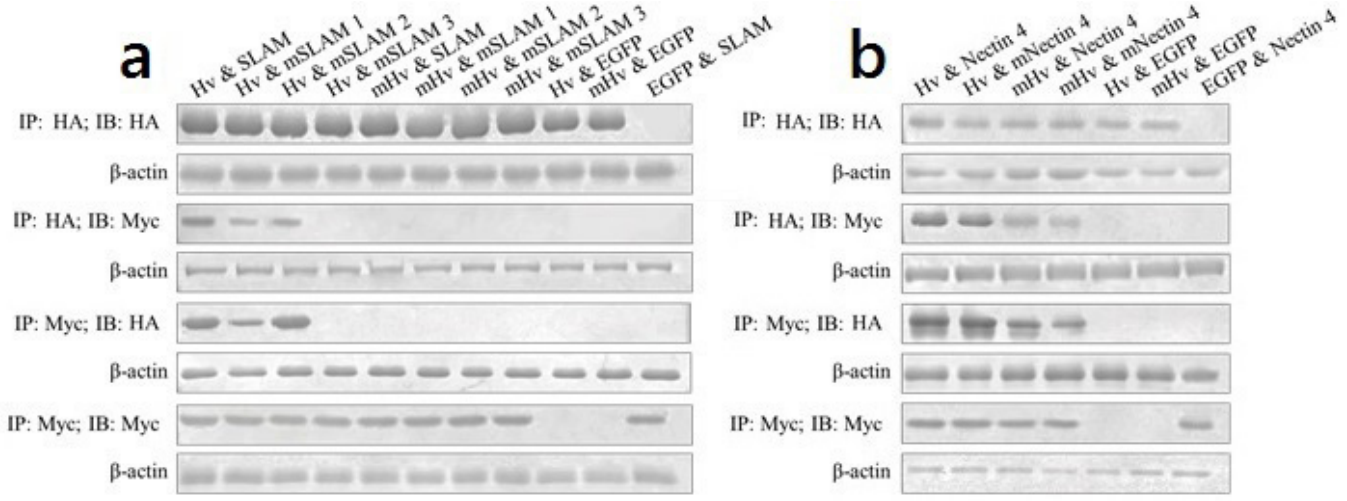

Fig. 5. Identification of the interaction between PPRV H and receptors by co-IP assay (a) The interaction of PPRV H with SLAM or its three mutants in CHO cells. (b) The interaction of PPRV H with Nectin 4 or mNectin 4 in CHO cells.

Table 2. The calibrated ratios of PPRV H interaction with SLAM and site-directed mutants determined by co-IP

Group	IP: Anti-HA	IP: Anti-HA	IP: Anti-Myc	IP: Anti-Myc
	IB: Anti-HA	IB: Anti-Myc	IB: Anti-HA	IB: Anti-Myc
Hv and SLAM	100.00%	100.00%	100.00%	100.00%
Hv and mSLAM1	97.84%	55.07%	36.99%	83.78%
Hv and mSLAM2	93.88%	89.50%	59.29%	88.22%
Hv and mSLAM3	104.68%	0.00%	0.00%	108.74%
mHv and SLAM	91.97%	0.00%	0.00%	118.61%
mHv and mSLAM1	92.71%	0.00%	0.00%	113.50%
mHv and mSLAM2	90.67%	0.00%	0.00%	120.19%
mHv and mSLAM3	93.83%	0.00%	0.00%	117.74%
Hv and EGFP	90.07%	0.00%	0.00%	0.00%
mHv and EGFP	90.49%	0.00%	0.00%	0.00%
EGFP and SLAM	0.00%	0.00%	0.00%	101.59%

which is consistent with the molecular simulation results [12]. It should be noted that the mSLAM1 protein bound to PPRV Hv with a very weak intensity, and the coprecipitation ability of Hv–mSLAM1 interaction was remarkably decreased to 36.99% of the WT level. The suggestion that the mutated amino acids (I61P, H62A, I210P A211R, S226A and R227A) in mSLAM1 have a crucial role in PPRV H binding to SLAM is in agreement with previous findings [14, 29–31]. Computational analysis showed that K77 and E123 in human and canine SLAM play pivotal roles in binding to the H protein of MV and CDV [16, 42, 43]. The two residues are known to be well conserved among the reported mammalian SLAMs. Nine amino acid residues in PPRV H (R389, L464, I498, R503, R533, Y541, Y543, F552 and Y553) were previously predicted to play pivotal roles in binding to SLAM [12]. Among these residues, four (R503, R533, Y543 and F552) were predicted to have and did show strong attractive interactions with SLAM [12, 16]. It should be noted that the amino acids at position 503 of PPRV H and MV H proteins are different, being arginine and propeller acid, respectively. Furthermore, the virological experiments verified that the R533 of MV H is essential for binding to SLAM [44, 45]. The present study showed the mHv protein lost binding activity to the WT and mutated SLAM, and the interaction of mHv protein with SLAM was not detected by co-IP. Based on the results, we confirmed that amino acids at positions R389, L464, I498, R503, R533, Y541, Y543, F552 and Y553 of PPRV H protein and I61, H62, L64, K76, K78, E123, H130, I210, A211, S226 and R227 in caprine SLAM determine the specificity of the PPRV H–SLAM interaction. The key residues of caprine SLAM are located at the region of 21 sites that are shared by hosts susceptible to the specific morbillivirus species [28]. The apparent affinity of Hv–mSLAM2 interaction was similar to that of Hv–SLAM. It would be interesting to experimentally assess residues M67, E69, D73, K77, R85, F119 and S121 of caprine SLAM and R191, D505, D507, D530 and R556 of PPRV H protein.

Table 3. The calibrated ratios of PPRV H interaction with Nectin 4 and mNectin 4 determined by by co-IP

Group	IP: Anti-HA	IP: Anti-HA	IP: Anti-Myc	IP: Anti-Myc
	IB: Anti-HA	IB: Anti-Myc	IB: Anti-HA	IB: Anti-Myc
Hv and **Nectin 4**	100.00%	100.00%	100.00%	100.00%
Hv and mNectin 4	90.30%	86.18%	70.50%	100.52%
mHv and Nectin 4	87.49%	34.33%	51.94%	90.66%
mHv and mNectin 4	92.84%	21.57%	30.36%	128.04%
Hv and EGFP	95.08%	0.00%	0.00%	0.00%
mHv and EGFP	101.47%	0.00%	0.00%	0.00%
EGFP and Nectin 4	0.00%	0.00%	0.00%	94.33%

Unfortunately, the key amino acid residues of the PPRV Hv–Nectin 4 interaction were not obtained in the present study. The PPRV Hv protein showed a strong attractive affinity (K_D=1.79×10^{-6} M) with the mutant mNectin 4; the coprecipitation ability remained above 70.5% of the WT level. The mutated sites of mNectin 4 were determined according to the predicted amino acids of PPRV H–Nectin 4 interaction by our research team (unpublished data). The mutated residues of caprine Nectin 4 were completely inconsistent with the predicted sites of human Nectin 4 interaction with MV H protein [16]. We could not rule out the possibility that this result was caused by the inaccuracy of mutant amino acids in the caprine Nectin 4 protein. The PPRV mHv protein bound to Nectin 4 with medium intensity (K_D=2.11×10^{-5} M) and 51.94% of the WT coprecipitation level or less. However, three residues of PPRV Hv, L464, Y541 and Y543, were the key amino acids of the MV H–Nectin 4 interaction [11, 16, 40]. The mutation at position 543 of MV H could result in the loss of binding activity with Nectin 4 [41, 46]. It is suggested that the mutated residues L464, Y541 and Y543 of PPRV Hv protein also play critical roles for interaction with caprine Nectin 4. The next step is to study the key amino acids involved in the interaction between PPRV H protein and caprine Nectin 4 further.

All in all, the amino acid residues R389, L464, I498, R503, R533, Y541, Y543, F552 and Y553 of PPRV H protein and I61, H62, L64, K76, K78, E123, H130, I210, A211, S226 and R227 in caprine SLAM were found to determine the specificity of the PPRV H–SLAM interaction. Although the key residues of PPRV H protein interacting with Nectin 4 were not confirmed, the present results lay a foundation for further study. Further along, the identified amino acids residues may be useful targets for developing peptide-based vaccines and inhibitors (antiviral drugs) against PPR.

METHODS

Plasmids and reagents

The recombinant plasmids pET30a-Hv (GenBank accession no. X74443), pET30a-SLAM (GenBank accession no. DQ228869) and pET30a-Nectin 4 (GenBank accession no. XP_004002729) and the vectors pCMV-Myc and pCMV-HA were provided by the Lanzhou Veterinary Research Institute of the Chinese Academy of Agricultural Sciences and were used to construct eukaryotic expressing plasmids. *Escherichia coli* DH5α, T4 DNA ligase and all restriction enzymes were purchased from TaKaRa (PR China). QIAprep spin Miniprep was from Qiagen. DMEM and F12K were purchased from HyClone (USA). Lipofectamine 3000 was from Invitrogen. Foetal bovine serum (FBS) was purchased from Gibco BRL Life Tech. The Pierce BCA Protein Assay kit and the Pierce Protein A/G Magnetic Beads kit were purchased from Thermo Fisher Scientific (USA). The microarray chips were roducts of Betterways, Inc. Biotin and streptavidin were purchased from Sigma (USA). Anti-HA, anti-Myc and anti-β-actin monoclonal antibody were purchased from Abcam (USA). The HRP-coupled secondary antibodies were products of Bioss (PR China) and the DAB HRP colour development kit was a Beyotime product (PR China).

Table 4. The site-directed mutants

WT amino Acids→mutated amino acids				
mSLAM1	**mSLAM2**	**mSLAM3**	**mNectin4**	**mHv**
61: I→P	64: L→N	62: H→A	58: G→R	389: R→A
62: H→A	67: M→N	64: L→N	63: Q→A	464: L→N
210: I→P	69: E→A	76: K→A	63: Q→A	498: I→P
211: A→R	73: D→A	78: K→A	84: K→A	503: R→A
226: S→A	85: R→A	123: E→A	131: F→N	533: R→A
227: R→A	119: F→N	130: H→A	132: P→A	541: Y→N
	121: S→A		136: F→N	543: Y→N
	130: H→A			552: F→N
				553: Y→N

Construction of eukaryotic expression vectors

The mutants mHv, mSLAM1, mSLAM2, mSLAM3 and mNectin 4 were generated based on a backbone of PPRV H (Nigeria 75/1), capra hircus SLAM (DQ228869) and ovis aries Nectin-4 (XP_004002729) protein in combination with the virological and predictive reports [11, 12, 14, 29–31, 40]. The site-directed mutants are shown in Table 4. Hv and mHv were introduced into pCMV-HA plasmid with HA and His tags; receptors and mutants were cloned into pCMV-Myc plasmid with Myc and His tags. The clones were verified by double digestion with corresponding restriction enzymes and sequencing

Cell culture and transfection

HEK293 cells and CHO-K1 were obtained from the Shanghai Institutes for Biological Sciences (SIBS, PR China). HEK293 cells were grown in DMEM and supplemented with 10% FBS and 1% penicillin/streptomycin (Thermo Scientific, USA). CHO-K1 cells were cultured in F12K supplemented with 5% FBS, 100 U ml^{-1} penicillin and 100 U ml^{-1} streptomycin at 37 °C in a humidified 5% CO_2 incubator.

For the production of recombinant proteins, HEK293 cells were transiently transfected with plasmids using Lipofectamine 3000 according to the manufacturer's instructions. The cells were cultured with 293 expression medium in a disposable flask (Thermo Fisher Scientific, USA) that was shaken at 110 r.p.m. using a rotary shaker for 6 d at 37 °C in a humidified 5% CO_2 incubator.

For immunoprecipitation, CHO cells were seeded into six-well plates to confluence. The different combinations of Hv–HA, mHv–HA, SLAM–Myc, Nectin 4–Myc, mSLAM1–Myc, mSLAM2–Myc, mSLAM3–Myc, mNectin 4–Myc or pcDNA3.1–EGFP were co-transfected using Lipofectamine 3000 as instructed by the manufacturer. Forty-eight hours

after transfection, the cells were lysed and subjected to immunoprecipitation.

Protein purification

The culture medium of transfected HEK293 cells was harvested and centrifuged, and then the supernatant was filtered through a 0.22 µm membrane filter (Merck Millipore, Germany). The expressed proteins were purified through dialysis (25 mM Tris, 150 mM NaCl, pH8.0) and Ni-IDA chromatography (Detai Biologics, PR China). The purified proteins were separated by SDS-PAGE and then analysed by Western blot, and the protein concentration was estimated using the Pierce BCA Protein Assay kit. The protein samples were stored in PBS at −80 °C.

Surface plasmon resonance imaging

Binding assays were performed using the Berthold bScreen LB 991 Label-free Microarray System (Berthold Technologies, Germany) according to the manufacturer's instructions. All of the reactions were performed at 4 °C.

The fresh microarray chips were treated according to the standard operating procedure provided by the manufacturer. The microarray chips used in this experiment were coated with a 47.5 nM thick gold layer and received photo-cross-linker chemical modification. The purified samples and controls, diluted to print concentration in PBS buffer, were printed onto the chip surface with a Biodot AD-1520 Array Printer (BioDot, Inc., USA). Each sample was printed on four parallel chips. The biotin (positive control) and DMSO (negative control) interaction with streptavidin were used as system controls for the measurement of specific signals.

The printed chips were dried by a stream of nitrogen to evaporate the solvent in the sample dots. Subsequently, the sensor chips were quickly transferred to a UV spectroirradiator for a photo-cross-linking reaction. Then, the chips were exposed to UV irradiation in a UV chamber (Amersham Life Science, USA). The irradiation programme was as follows: 100 µW cm^{-2}, 2 min; pause 2 min; 100 µW cm^{-2}, 2 min; pause 2 min; 25 µW cm^{-2}, 15 min. The chips were subsequently rinsed with dimethylformamide, ethanol and distilled water for 15 min to remove non-specifically adsorbed compounds and were dried under a stream of nitrogen. Two more sensor chips were prepared as replicates. The chips were inserted into the SPRi instrument for measurement.

All protein samples were injected at a rate of 0.5 µL s^{-1}. PBS (pH=7.0) was used as both an analyte and running buffer. Additionally, the solvent (PBS) for proteins was also tested. At the end of the affinity test, PBS was crosswise tested with all proteins on the chip as the background noise control.

During the SPRi test, the surface was first primed three times with HBS-EP running buffer [containing 10 mM HEPES, pH 7.0, 150 mM NaCl, 3 mM EDTA and 0.005% (v/v) of P20 surfactant] at a rate of 2 µL s^{-1} for 40 s and one time with running buffer (1×PBS) at a rate of 2 µL s^{-1} for 40 s. The eight proteins flowed as analytes were diluted separately with PBS to five different concentrations (200, 400, 800, 1600 and 3200 nM). A solution of 10 mM glycine–HCl (pH 2.0) was used to regenerate the surface at a rate of 2 µLs^{-1}. Each cycle of sample analysis consisted of a 600 s association phase, a 360 s dissociation phase and a 300 s regeneration phase. The raw sensorgrams and affinity parameters of the binding process of ligands and analytes were recorded in real time. The response unit (RU) of surface resonance was compared to determine the different binding affinities between each sample dot. The interaction parameters, the association rate constant (k_a/k_{on}), the dissociation rate constant (k_d/k_{off}), and the equilibrium dissociation constant (K_D, k_d/k_a), were processed and analysed using the data analysis software of the bScreen LB 991 unlabelled microarray system according to a single-site binding model (1:1 Langmuir binding) with mass transfer limitations for binding kinetics determination. All binding curves were normalized by subtracting the background signal.

Co-immunoprecipitation assay

At 48 h post-transfection, cells were harvested and washed twice with ice-cold PBS (pH 7.4) and then lysed with RIPA lysis buffer (50 mM Tris, 150 mM NaCl, 1% NP-40, 0.5% sodium deoxycholate and 0.1% SDS) for 30 min on ice. The lysates were centrifuged at 12000 r.p.m. for 30 min at 4 °C and the supernatants were immunoprecipitated using a Pierce Protein A/G Magnetic Beads kit (Thermo Fisher scientific). Rabbit anti-HA and mouse anti-Myc tag monoclonal antibodies (Abcam) were covalently linked to protein A/G magnetic beads by disuccinimidyl suberate (DSS; Thermo Fisher), respectively. Co-IPs with the antibody-coupled resin were performed at 4 °C overnight. The following day, the beads were washed and the bound protein was eluted. The elution fractions were separated on SDS-PAGE for Western blot analysis.

Western blot and data analysis

Samples were subjected to SDS-PAGE and transferred to a nitrocellulose membrane. The membranes were incubated with anti-HA, anti-Myc, or anti-β-actin, followed by appropriate HRP-conjugated secondary antibodies. The signals were visualized using the DAB HRP colour development kit. The relative expression of proteins of co-IP was analysed quantitatively using an Arrayit SpotLight Fluorescence Scanner and the AlphaView SA system (version 3.2.4.0, Cell Biosciences, Inc.)

Funding information
This work is supported by the National Research and Development Program of China (2016YFD0500108) and the National Natural Science and Foundation of China (NSFC, 31300142).

Conflicts of interest
The authors declare that there are no conflicts of interest.

References

1. Baron MD, Diallo A, Lancelot R, Libeau G. Peste des petits ruminants virus. *Adv Virus Res* 2016;95:1–42.

2. Albina E, Kwiatek O, Minet C, Lancelot R, Servan de Almeida R *et al*. Peste des petits ruminants, the next eradicated animal disease? *Vet Microbiol* 2013;165:38–44.
3. Banyard AC, Parida S, Batten C, Oura C, Kwiatek O *et al*. Global distribution of peste des petits ruminants virus and prospects for improved diagnosis and control. *J Gen Virol* 2010;91:2885–2897.
4. Kwiatek O*et al*. Asian lineage of peste des petits ruminants virus, Africa. *Emerg Infect Dis* 2011;17:1223–1231.
5. Muniraju M, Mahapatra M, Ayelet G, Babu A, Olivier G *et al*. Emergence of lineage IV peste des petits ruminants virus in Ethiopia: complete genome sequence of an Ethiopian isolate 2010. *Transbound Emerg Dis* 2016;63:435–442.
6. OIE-WAHIS. Peste des petits ruminants. retrieved from: annual animal health report, world animal health information database (WAHIS interface) – version 1, world organisation for animal health (OIE), Bulgaria 2018.
7. Baron MD, Diop B, Njeumi F, Willett BJ, Bailey D. Future research to underpin successful peste des petits ruminants virus (PPRV) eradication. *J Gen Virol* 2017;98:2635–2644.
8. Thomson GR, Fosgate GT, Penrith M-L. Eradication of transboundary animal diseases: can the rinderpest success story be repeated? *Transbound Emerg Dis* 2017;64:459–475.
9. Altan E, Parida S, Mahapatra M, Turan N, Yilmaz H. Molecular characterization of peste des petits ruminants viruses in the Marmara region of turkey. *Transbound Emerg Dis* 2019;66:865–872.
10. Colf LA, Juo ZS, Garcia KC. Structure of the measles virus hemagglutinin. *Nat Struct Mol Biol* 2007;14:1227–1228.
11. Hashiguchi T, Ose T, Kubota M, Maita N, Kamishikiryo J *et al*. Structure of the measles virus hemagglutinin bound to its cellular receptor SLAM. *Nat Struct Mol Biol* 2011;18:135–141.
12. Liang Z, Yuan R, Chen L, Zhu X, Dou Y. Molecular evolution and characterization of hemagglutinin (H) in peste des petits ruminants virus. *PLoS One* 2016;11:e0152587.
13. Navaratnarajah CK, Kumar S, Generous A, Apte-Sengupta S, Mateo M *et al*. The measles virus hemagglutinin stalk: structures and functions of the central fusion activation and membrane-proximal segments. *J Virol* 2014;88:6158–6167.
14. Hu C, Zhang P, Liu X, Qi Y, Zou T *et al*. Characterization of a region involved in binding of measles virus H protein and its receptor SLAM (CD150). *Biochem Biophys Res Commun* 2004;316:698–704.
15. Xu Q, Zhang P, Hu C, Liu X, Qi Y *et al*. Identification of amino acid residues involved in the interaction between measles virus Haemagglutin (MVH) and its human cell receptor (signaling lymphocyte activation molecule, SLAM). *J Biochem Mol Biol* 2006;39:406–411.
16. Xu F, Tanaka S, Watanabe H, Shimane Y, Iwasawa M *et al*. Computational analysis of the interaction energies between amino acid residues of the measles virus hemagglutinin and its receptors. *Viruses* 2018;10:236.
17. Birch J, Juleff N, Heaton MP, Kalbfleisch T, Kijas J *et al*. Characterization of ovine Nectin-4, a novel peste des petits ruminants virus receptor. *J Virol* 2013;87:4756–4761.
18. Pawar RM, Raj GD, Kumar TM, Raja A, Balachandran C. Effect of siRNA mediated suppression of signaling lymphocyte activation molecule on replication of peste des petits ruminants virus in vitro. *Virus Res* 2008;136:118–123.
19. Mühlebach MD, Mateo M, Sinn PL, Prüfer S, Uhlig KM *et al*. Adherens junction protein Nectin-4 is the epithelial receptor for measles virus. *Nature* 2011;480:530–533.
20. Seki F, Ono N, Yamaguchi R, Yanagi Y. Efficient isolation of wild strains of canine distemper virus in Vero cells expressing canine SLAM (CD150) and their adaptability to marmoset B95a cells. *J Virol* 2003;77:9943–9950.
21. Pratakpiriya W, Seki F, Otsuki N, Sakai K, Fukuhara H *et al*. Nectin4 is an epithelial cell receptor for canine distemper virus and involved in neurovirulence. *J Virol* 2012;86:10207–10210.
22. Tatsuo H, Yanagi Y. The morbillivirus receptor SLAM (CD150). *Microbiol Immunol* 2002;46:135–142.
23. Cocks BG, Chang C-CJ, Carballido JM, Yssel H, de Vries JE *et al*. A novel receptor involved in T-cell activation. *Nature* 1995;376:260–263.
24. Bleharski JR, Niazi KR, Sieling PA, Cheng G, Modlin RL. Signaling lymphocytic activation molecule is expressed on CD40 ligand-activated dendritic cells and directly augments production of inflammatory cytokines. *J Immunol* 2001;167:3174–3181.
25. Ohgimoto S, Ohgimoto K, Niewiesk S, Klagge IM, Pfeuffer J *et al*. The haemagglutinin protein is an important determinant of measles virus tropism for dendritic cells *in vitro*. *J Gen Virol* 2001;82:1835–1844.
26. Wang N, Satoskar A, Faubion W, Howie D, Okamoto S *et al*. The cell surface receptor SLAM controls T cell and macrophage functions. *J Exp Med* 2004;199:1255–1264.
27. Ono N, Tatsuo H, Tanaka K, Minagawa H, Yanagi Y. V domain of human SLAM (CDw150) is essential for its function as a measles virus receptor. *J Virol* 2001;75:1594–1600.
28. Ohishi K, Ando A, Suzuki R, Takishita K, Kawato M *et al*. Host–virus specificity of morbilliviruses predicted by structural modeling of the marine mammal SLAM, a receptor. *Comp Immunol Microbiol Infect Dis* 2010;33:227–241.
29. Ohno S, Seki F, Ono N, Yanagi Y. Histidine at position 61 and its adjacent amino acid residues are critical for the ability of SLAM (CD150) to act as a cellular receptor for measles virus. *J Gen Virol* 2003;84:2381–2388.
30. Yanagi Y, Takeda M, Ohno S, Hashiguchi T. Measles virus receptors. *Curr Top Microbiol Immunol* 2009;329:13–30.
31. Sarkar J, Balamurugan V, Sen A, Saravanan P, Sahay B *et al*. Sequence analysis of morbillivirus CD150 receptor-signaling lymphocyte activation molecule (SLAM) of different animal species. *Virus Genes* 2009;39:335–341.
32. Kurita S, Ogita H, Takai Y. Cooperative role of nectin-nectin and nectin-afadin interactions in formation of nectin-based cell-cell adhesion. *J. Biol. Chem.* 2011;286:36297–36303.
33. Takai Y, Miyoshi J, Ikeda W, Ogita H. Nectins and nectin-like molecules: roles in contact inhibition of cell movement and proliferation. *Nat Rev Mol Cell Biol* 2008;9:603–615.
34. Ogita H, Takai Y. Nectins and nectin-like molecules: roles in cell adhesion, polarization, movement, and proliferation. *IUBMB Life* 2006;58:334–343.
35. Takai Y, Nakanishi H. Nectin and afadin: novel organizers of intercellular junctions. *J Cell Sci* 2003;116:17–27.
36. Delpeut S, Noyce RS, Richardson CD. The V domain of dog PVRL4 (Nectin-4) mediates canine distemper virus entry and virus cell-to-cell spread. *Virology* 2014;454-455:109–117.
37. Meng X, Deng R, Zhu X, Zhang Z. Quantitative investigation of the direct interaction between hemagglutinin and fusion proteins of peste des petits ruminant virus using surface plasmon resonance. *Virol J* 2018;15:21.
38. Crennell S, Takimoto T, Portner A, Taylor G. Crystal structure of the multifunctional paramyxovirus hemagglutinin-neuraminidase. *Nat Struct Biol* 2000;7:1068–1074.
39. Hashiguchi T, Kajikawa M, Maita N, Takeda M, Kuroki K *et al*. Crystal structure of measles virus hemagglutinin provides insight into effective vaccines. *Proc Natl Acad Sci U S A* 2007;104:19535–19540.
40. Zhang X, Lu G, Qi J, Li Y, He Y *et al*. Structure of measles virus hemagglutinin bound to its epithelial receptor Nectin-4. *Nat Struct Mol Biol* 2013;20:67–72.
41. Tahara M, Takeda M, Shirogane Y, Hashiguchi T, Ohno S *et al*. Measles virus infects both polarized epithelial and immune cells by using distinctive receptor-binding sites on its hemagglutinin. *J Virol* 2008;82:4630–4637.
42. Ohishi K, Suzuki R, Maruyama T. Host-virus specificity of the morbillivirus receptor, SLAM, in marine mammals: risk assessment of infection based on three-dimensional models. In: Romero A, Keith EO (editors). *New Approaches to the Study of Marine Mammals*. Rijeka, Croatia: InTech; 2014. pp. 123–204.

43. Khosravi M, Bringolf F, Röthlisberger S, Bieringer M, Schneider-Schaulies J *et al*. Canine distemper virus fusion activation: critical role of residue E123 of CD150/SLAM. *J Virol* 2016;90:1622–1637.
44. Masse N, Ainouze M, Neel B, Wild TF, Buckland R *et al*. Measles virus (mV) hemagglutinin: evidence that attachment sites for mV receptors SLAM and CD46 overlap on the globular head. *J Virol* 2004;78:9051–9063.
45. Vongpunsawad S, Oezgun N, Braun W, Cattaneo R. Selectively receptor-blind measles viruses: identification of residues necessary for SLAM- or CD46-induced fusion and their localization on a new hemagglutinin structural model. *J Virol* 2004;78:302–313.
46. Leonard VH, Sinn PL, Hodge G, Miest T, Devaux P *et al*. Measles virus blind to its epithelial cell receptor remains virulent in rhesus monkeys but cannot cross the airway epithelium and is not shed. *J Clin Invest* 2008;118:2448–2458.